APPLIED AND ENVIRONMENTAL MICROBIOLOGY, Aug. 2003, p. 4794–4805 Vol. 69, No. 8
0099-2240/03/$08.00+0 DOI: 10.1128/AEM.69.8.4794–4805.2003

CynD, the Cyanide Dihydratase from *Bacillus pumilus*: Gene Cloning and Structural Studies

Dakshina Jandhyala,[1] Mark Berman,[2,3] Paul R. Meyers,[3] B. Trevor Sewell,[2] Richard C. Willson,[1,4] and Michael J. Benedik[1]*

Department of Biology and Biochemistry[1] and Department of Chemical Engineering,[4] University of Houston, Houston, Texas 77204, and Electron Microscopy Unit[2] and Department of Molecular and Cell Biology,[3] University of Cape Town, Cape Town, South Africa

Received 2 December 2002/Accepted 2 May 2003

The cyanide dihydratase in *Bacillus pumilus* was shown to be an 18-subunit spiral structure by three-dimensional reconstruction of electron micrographs of negatively stained material at its optimum pH, 8.0. At pH 5.4, the subunits rearrange to form an extended left-handed helix. Gel electrophoresis of glutaraldehyde cross-linked enzyme suggests that the fundamental component of the spiral is a dimer of the 37-kDa subunit. The gene was cloned, and the recombinant enzyme was readily expressed at high levels in *Escherichia coli*. Purification of the recombinant enzyme was facilitated by the addition of a C-terminal six-histidine affinity purification tag. The tagged recombinant enzyme has K_m and V_{max} values similar to those published for the native enzyme. This is the first cyanide dihydratase from a gram-positive bacterium to be sequenced, and it is the first description of the structure of any member of this enzyme class. The putative amino acid sequence shares over 80% identity to the only other sequenced cyanide dihydratase, that of the gram-negative *Pseudomonas stutzeri* strain AK61, and is similar to a number of other bacterial and fungal nitrilases. This sequence similarity suggests that the novel short spiral structure may be typical of these enzymes. In addition, an active cyanide dihydratase from a non-cyanide-degrading isolate of *B. pumilus* (strain 8A3) was cloned and expressed. This suggests that *cynD*, the gene coding for the cyanide dihydratase, is not unique to the C1 strain of *B. pumilus* and is not a reflection of its origin at a mining waste site.

Various industrial processes, notably leach mining, metal finishing, and electroplating, generate large amounts of cyanide-containing waste. As a potent inhibitor of cytochrome oxidase, cyanide is toxic to aerobic organisms, and extended exposure of humans to cyanide has been linked to certain neuropathies (29, 34). Therefore, cyanide-containing waste must be detoxified prior to its deposition into the environment. Conventional methods used for cyanide detoxification, such as alkaline chlorination, use hazardous chemicals that are both costly and generate toxic by-products (16, 36). Microorganisms, however, have been shown to utilize and degrade cyanide, thereby providing opportunities to develop new biologically based methods for the detoxification of cyanide-containing waste (8, 17).

There are a number of enzymes whose ability to degrade or modify cyanide has been described. Nitrilases are a group of enzymes that hydrolyze nitriles (R—C≡N), of which cyanide (HCN) is the simplest, to ammonia and the corresponding carboxylic acid (R—COOH) (22). Cyanide-degrading enzymes can be of two types, whose reactions are shown in Fig. 1. The first, the cyanide dihydratases, comprise a group of bacterial enzymes that include those from *Alcaligenes xylosoxidans* subsp. *denitrificans* DF3, *Bacillus pumilus* C1, and *Pseudomonas stutzeri* AK61 (12, 20, 32). All these behave as true nitrilases, converting cyanide directly to formate and ammonia (12, 20, 32). The enzymes in the other group, the cyanide hydratases, which hydrolyze cyanide to formamide, are all of fungal origin. These enzymes are more closely related to the nitrilases than to the metal-containing nitrile hydratases (22). The best characterized of the cyanide hydratases are those from *Gloeocercospora sorghi* and *Fusarium lateritium* (5, 31).

Of the cyanide dihydratases, only the gene encoding the enzyme from *P. stutzeri* AK61 has been sequenced (33). Its predicted amino acid sequence shares identity at levels of 35 and 28%, respectively, with the cyanide hydratases of *G. sorghi* and *F. lateritium*, and even greater identity (>40%) is shared with some non-cyanide-specific nitrilases. These hydrolytic enzymes do not require additional cofactors or substrates and function over a wide substrate concentration, thereby making them good candidates for use in the bioremediation of cyanide. In fact, *F. lateritium* and *A. xylosoxidans* subsp. *denitrificans* have been patented for use as granular biocatalysts for the detoxification of cyanide-containing waste (13, 25).

The cyanide-degrading bacterium *B. pumilus* C1 was isolated from a cyanide-containing wastewater dam belonging to a South African mining company (19). The enzyme responsible for the cyanide-degrading activity of this *B. pumilus* strain has been characterized biochemically, but there is little data concerning its structure, amino acid sequence, or its ability to be expressed in a heterologous host (20, 21). In this study, we describe the quaternary structure, cloning, sequencing, and expression in *Escherichia coli* of the gene encoding cyanide dihydratase in *B. pumilus* C1 as well as that of a homologous gene from a non-cyanide-degrading isolate, *B. pumilus* 8A3.

* Corresponding author. Mailing address: Department of Biology and Biochemistry, University of Houston, Houston, TX 77204-5001. Phone: (713) 743-8377. Fax: (713) 743-8351. E-mail: benedik@uh.edu.

MATERIALS AND METHODS

Bacterial strains and plasmids. The plasmids and strains used in this study are described in Table 1. *E. coli* strain MB1547 was the host strain used for plasmid

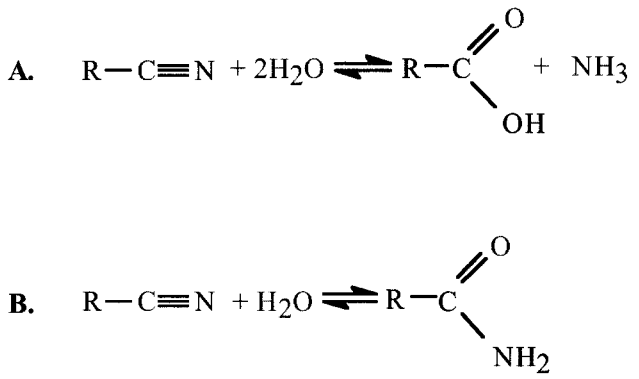

FIG. 1. The hydrolysis of nitriles by nitrilases occurs by one of two routes. The nitrilase branch of the nitrilase superfamily catalyzes the hydrolysis of nitriles to ammonia and the corresponding carboxylic acid (A), while cyanide hydratases and the metal-containing nitrile hydratases convert nitriles to the corresponding amide (B).

construction. The *B. pumilus* strain C1 has been previously described (19), and *B. pumilus* 8A3 was obtained from the *Bacillus* Genetic Stock Center (Ohio State University). The plasmid pBS(KS+) was used for the routine cloning of PCR products. The temperature-sensitive plasmid pE194 was used in the construction of p3022, which in turn was used as a delivery system for gene replacement in *B. pumilus* C1. Plasmid p3019 carries a 539-bp internal fragment of the *B. pumilus* C1 cyanide dihydratase gene cloned in the *Eco*RV site of pBS(KS+).

Culture media and reagents. Unless otherwise mentioned, all strains were grown on Luria broth (LB). Antibiotics were added to concentrations of 100 μg of ampicillin per ml, 30 μg of chloramphenicol per ml, 25 μg of kanamycin per ml, and a mixture of 1 μg of erythromycin plus 25 μg of lincomycin per ml for selection in *Bacillus* species. 5-Bromo-4-chloro-3-indolyl-β-D-galactopyranoside (X-Gal) was used at a concentration of 20 to 30 μg/ml. *B. pumilus* C1 strains were grown with 1 μg of $MnCl_2$/ml, except as stated below, for induction of cyanide dihydratase activity (19).

Preparation of native cyanide dihydratase from *B. pumilus*. One milliliter of a stock culture of *B. pumilus* C1 cells was added to each of six 2-liter flasks containing 250 ml of LB and 25 μM $MnSO_4$ and grown for 12 h at 30°C with shaking. Cells were harvested by centrifugation for 10 min at 7,740 × *g*, resuspended in cold 10 mM Tris–50 mM NaCl (pH 8), and washed twice. They were then resuspended in 1/40 volume of the same buffer containing 1 mM EDTA, 0.5 μg of leupeptin/ml, and 2 μg of aprotinin/ml. The cells were ruptured by sonication for 3 min (5-s pulse, 15-s pause) in a Virsonic Digital 475 ultrasonicator (Virtis) with a blunt 0.5-in. horn. This and all subsequent steps were performed at 4°C. The lysate was centrifuged for 30 min at 27,210 × *g*.

The cleared lysate was filtered through a 0.45-μm-pore-size Millipore membrane and loaded onto a Whatman DE52 anion exchange column (1.17 by 50 cm), preequilibrated in 10 mM Tris–50 mM NaCl (pH 8). The column was washed thoroughly with loading buffer, after which a linear gradient from 50 to 250 mM NaCl in 10 mM Tris (pH 8) was applied over 2 column volumes. Active fractions, assayed by the picric acid method of Fisher and Brown as described below (10), were pooled, concentrated to 0.8 ml in an Amicon ultrafiltration cell using a PM10 membrane, and applied to a prepacked Sephacryl 300 HR 16/60 gel filtration column (AP Biotech). Elution was in 10 mM Tris–360 mM NaCl (pH 8) by gravity flow (2.6 cm/h). The pooled active fractions were concentrated by ultrafiltration.

Electron microscopy. The purified enzyme was diluted 1:40 in 10 mM triethanolamine–50 mM NaCl (pH 8) to a final protein concentration of 0.15 mg/ml. A carbon-coated copper grid was placed on a droplet of this enzyme preparation for 10 min, blotted, and then stained with 2% uranyl acetate for 3 min. The grid was then blotted and air dried. Stocks of cyanide dihydratase were diluted 25-fold in 10 mM citrate–360 mM NaCl (pH 5.4) and then concentrated to 0.4 mg/ml by ultrafiltration. This was then loaded onto the Sephacryl 300 HR gel filtration column, which was preequilibrated with 10 mM citrate–360 mM NaCl (pH 5.4), and eluted with the same buffer. Protein from the void volume was collected. This was diluted to 0.02 mg/ml in 10 mM citrate–50 mM NaCl (pH 5.4) and applied to a carbon-coated copper grid. Staining with uranyl acetate was carried

TABLE 1. Bacterial strains and plasmids

Strain or plasmid	Description or genotype	Reference
Strains		
E. coli		
BL21(DE3) pLysS	F^- *ompT hsdS*$_B$ *gal dcm* (DE3) Cm^r	Novagen
MB1547	*supE thi hsdΔ5* Δ(*lac-proAB*) Δ*endA*/*F'*[*traD36 proAB lacI*^{q} *lacZΔM15*]	Lab stock
MB2890	BL21(DE3) pLysS p2890	This work
MB2899	BL21(DE3) pLysS p2899	This work
MB3033	BL21(DE3) pLysS p3033	This work
B. subtilis		
168	*thr-5 trpC2*	4
BGSC1E18	168 pE194	35
B. pumilus		
C1	$CynD^+$ phenotype[a]	19
BGSC#8A3	Wild-type isolate	27
MB3025	C1 p3022	This work
MB3025-1	C1 *cynD*::p3022 (51°C integrant) $CynD^-$ phenotype	This work
Plasmids		
pBS(KS+)	Ap^r *E. coli* cloning vector	Stratagene
pET-26b	Kan^r *E. coli* expression vector	Novagen
pE194	Gram-positive temperature-sensitive plasmid	35
p2890	pET26b *cynD*$_{C1}$ as a *Nde*I-*Xho*I insertion	This work
p2899	pET26b *cynD*$_{C1\text{-}his}$ as a *Nde*I-*Xho*I insertion[b]	This work
p3026	*Sac*I fragment flanking the p3022 insertion into the chromosome of *B. pumilus* C1 in pBS(KS+)	This work
p3019	pBS(KS+)-*cynD*$_{539}$-*Eco*RV[c]	This work
p3022	P3019 as a *Pst*I-*Xba*I insertion in pE194; dual-origin shuttle vector	This work
p3033	pET26b *cynD*$_{8A3}$ as a *Nde*I-*Xho*I insertion	This work

[a] cynD refers to the gene encoding cyanide dihydratase or the cyanide-degrading phenotype.
[b] *cynD*$_{his}$ refers to the C1 cyanide dihydratase gene carrying a C-terminal six-histidine tag.
[c] *cynD*$_{539}$ is the 539-bp internal fragment of the *B. pumilus* C1 cyanide dihydratase gene which was generated by degenerate-primer PCR.

TABLE 2. Primer sequences

Primer name	Sequence[a]
Pum-7	GCI GCI GCI GTI CAR GCI GCI CCI GTI TAY
Int-1	GGC CAI GCI GCI ACR TGI ACY TGY TC
Out-2	AAT GCT TCT GGG AAT GCC ACA AGC
Out-3	TGG CGG TTC TCT CTA TTT AGC TCA G
Pum-NdeI	CAT ATG ACA AGT ATT TAC CCA AAG TTT C
Pum-XhoI	GTA GCC TCG AGA GAA GGA TCA TAC GCC ATT TCT ACA C
Pum-His	GAC TTA CTC GAG AAC TTT TTC TTC CAG TAT ACC C

[a] Sequences are 5′ to 3′; I, inosine; Y, C or T; R, G or A.

out as above. In the case of the shadowed specimens, unidirectional shadowing was performed with Pt-C from an electron beam evaporator (Balzers Union). The thickness of the coating was too thin to be measurable on the quartz crystal monitor. Micrographs were taken by the minimum dose technique at 50,000× magnification on a JEOL 1200CX.

Three-dimensional reconstruction. Images were digitized on a Leafscan 45 linear CCD scanner (Ilford Ltd, Cheshire, United Kingdom) with a step size of 10 μm, which corresponds to a pixel size of 2.0 Å on the specimen. For each image, adjacent pixels were averaged to reduce the resolution to 4.0 Å per pixel. Particle selection was performed with Ximdisp (6). A total of 13,019 particles were selected in 80- by 80-pixel areas, band pass filtered between 250 and 15 Å without CTF correction, and normalized to the same mean and standard deviation with SPIDER (11). The single-particle images were classified into 84 classes using the AP CA function (23) in SPIDER. Membership of these classes was refined by several cycles of sorting by using the AP NQ function (23) and the exclusion of poorly matching images. The angular relationship of the 40 most populous classes was determined by the common lines method by using the OP function (24). A starting model was created by back projection according to these angular relationships. A set of 84 projection angles, equally spaced at 15° intervals, was created with the VO EA function. Projections of the starting model were then made with these angles. Multiple cycles of refinement were performed, comprising (i) sorting with AP NQ against the projected templates, (ii) averaging the classes thus determined, (iii) back projecting (using the BP RP function) the class averages to create a model, and (iv) reprojecting this model to create the next generation of templates. After 40 cycles, it became apparent that the structures had global twofold axes. The orientation of the twofold axis was determined, and the model was relocated in the box so that the twofold axis was located along the center of the box parallel to the *x* axis. In 98 subsequent cycles of refinement, the twofold symmetry was imposed by rotating about the *x* axis and adding the structure thus formed to the original. The procedure was terminated when no further changes in the map were visible. The resolution was determined by dividing the images into two equally populated sets, reconstructing separately, and determining the Fourier shell correlation in shells of 1-pixel thickness.

Cross-linking with glutaraldehyde and SDS-polyacrylamide gel electrophoresis (PAGE). One microliter of purified enzyme stock was diluted to 31 μl with glutaraldehyde (25% EM grade; Agar Scientific, Ltd, Essex, United Kingdom) at the specified concentration made up in 10 mM triethanolamine–50 mM NaCl (pH 8.0) to give a final enzyme concentration of 0.2 mg/ml. Reactions were performed at room temperature for 75 min. Reactions were terminated by the addition of 6 μl of 0.5 M glycine. Eight microliters of sodium dodecyl sulfate (SDS) reducing buffer (62.5 mM Tris-HCl [pH 6.8], 20% glycerol, 2% SDS, 5% β-mercaptoethanol) was added to the reaction mixture, and it was boiled for 2 min. The entire sample was loaded onto a 10% acrylamide–0.05% bisacrylamide gel. The glutaraldehyde-treated sample was shown by matrix-assisted laser desorption ionization–time of flight (MALDI-TOF) to contain a range of polymers with a maximum length of 9 repeats (data not shown).

MALDI-TOF analysis of *B. pumilus* C1 cyanide dihydratase. After gel electrophoresis, the CynD bands of approximately 15 mm^3 were excised from polyacrylamide gels and were prepared according to the protocol obtained from the Yale University School of Medicine HHMI Biopolymer/Keck Foundation Biotechnology Resource Laboratory website (http://info.med.yale.edu/wmkeck/geldig3.htm). The gel slices were washed with 250 μl of 50% acetonitrile for 5 min, 250 μl of 50% acetonitrile–50 mM NH_4HCO_3 for 30 min, and 250 μl of 50% acetonitrile–10 mM NH_4HCO_3 for 30 min and then vacuum centrifuged to complete dryness. Protein was digested in the gel with 0.1 μg of trypsin and dissolved in 15 μl of 10 mM NH_4HCO_3 for 10 min; then, 20 μl of 10 mM NH_4HCO_3 was added, and the sample was incubated overnight at 37°C.

Following this procedure, 1 μl of the in-gel trypsin digest was extracted from the gel by centrifugation, mixed with an equal volume of the matrix α-cyano-4-hydroxycinnamic acid (MW 189.17) or sinapinic acid (MW 224.21), and placed on a sample grid to dry. This was then analyzed using a Perseptive Biosystems DE-PRO MALDI-TOF spectrometer.

Genomic and plasmid DNA preparation. Genomic DNA from *B. pumilus* was prepared with the Bactozol kit (Molecular Research Center, Inc., Cincinnati, Ohio). Plasmid DNA from *B. pumilus* C1 or *Bacillus subtilis* 168-derived strains was prepared by the alkaline lysis method (1, 3). Plasmid DNA from *E. coli* strains was prepared using the Wizard Plus Miniprep DNA purification system (Promega, Madison, Wis.).

Conditions for degenerate primer PCR. A general two-step PCR method using Platinum *Taq* DNA Polymerase High Fidelity (Invitrogen Life Technologies, Carlsbad, Calif.) was employed for the PCR amplification of cyanide dihydratase gene segments from genomic DNA of *B. pumilus* C1 with the degenerate oligonucleotide primers listed in Table 2. This method consisted of 10 cycles with an annealing temperature of 50°C followed by 25 cycles with an annealing temperature of 58°C. For all 35 cycles, the annealing time was kept at 30 s, the elongation time was set for 1 min at 68°C, and denaturation was set at 96°C for 30 s.

Inverse PCR. Genomic DNA from *B. pumilus* C1 was digested with *Taq*I (New England Biolabs) and ligated using T4 DNA ligase (New England Biolabs). DNA concentrations less than 10 μg/ml were used to favor intramolecular ligation events. The ligation products were then used as template DNA for PCRs using the two-step PCR method described above. Agarose gel electrophoresis was used to visualize PCR products, which were purified either directly from the agarose gel or by using Chromospin-200 columns (CLONTECH Laboratories, Inc.). The purified PCR products were then treated with T4 polymerase to create blunt ends, cloned into the *Eco*RV site of pBS(KS+), and analyzed by DNA sequencing.

Construction of p3022. The temperature-sensitive plasmid pE194 was prepared from *B. subtilis* BGSC1E18. Plasmid DNA was digested with *Pst*I and *Xba*I, the fragments were separated on a 0.7% agarose gel, and the larger 3,253-bp band was excised and purified. The plasmid p3019 was also digested with *Pst*I and *Xba*I and then ligated with the purified *Pst*I/*Xba*I fragment of pE194 to generate p3022. The ligation products were transformed into *E. coli* MB1547 and selected on ampicillin medium. Transformants were analyzed by restriction digestion as well as by the ability to confer erythromycin-lincomycin resistance on *B. subtilis* 168.

Transformation of *Bacillus* strains. Competent *B. subtilis* 168 cells were prepared and transformed by a modified version of previously referenced methods (7, 9). Transformation of plasmid DNA into *B. pumilus* C1 was done by electroporation. A fresh 100-ml culture was started in LB with a 100-fold dilution of an overnight *B. pumilus* C1 culture. This culture was incubated at 37°C with shaking at 250 rpm. When the optical density at 600 nm reached between 1.5 and 2.0, the cells were harvested by centrifugation. The pellet was washed three times with sterile cold double-distilled H_2O and resuspended in 1% of the original volume of sterile cold 30% polyethylene glycol (PEG) 6000. Electroporation of *B. pumilus* C1 was done with a BTX Electro cell manipulator 600 (ECM600). The resistance was set to 720 Ω, and the field strength was set to 12.5 kV/cm, with 0.5 to 1.0 μg of DNA added to 100 μl of cells in a BTX disposable cuvette P/N 620 (2-mm gap). Afterwards, the cells were diluted with 1 ml of SOC broth (2% tryptone, 0.5% yeast extract, 10 mM NaCl, 2.5 mM KCl, 10 mM $MgCl_2$, 20 mM glucose) and grown at 37°C with shaking (250 rpm) for 90 min. Selection for p3022 was performed on LB agar supplemented with erythromycin-lincomycin.

Cyanide dihydratase overexpression in *E. coli*. Cultures of MB2890 or MB2899 were grown at 30°C and 250 rpm overnight. Fresh cultures were started using 1/100 volume of an overnight culture and incubated at 30°C with shaking until the optical density at 600 nm approached 0.5. The cells were induced by the addition of isopropyl-β-D-thiogalactopyranoside (IPTG) to a final concentration

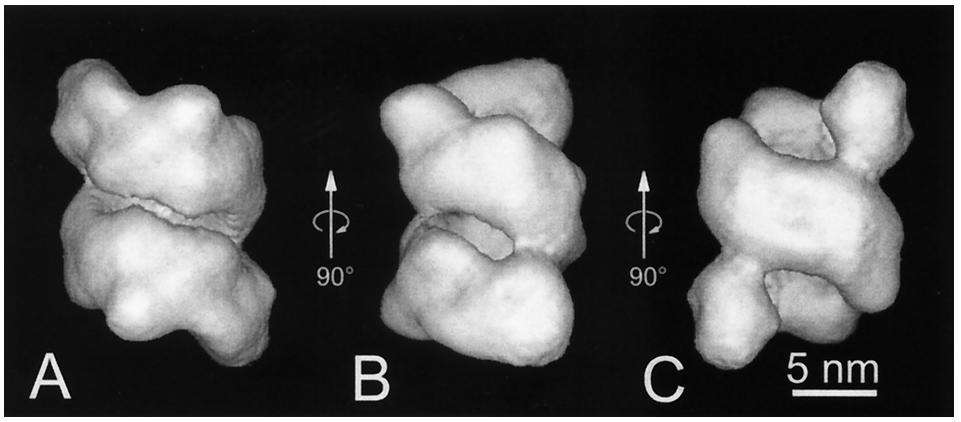

FIG. 2. Three-dimensional reconstruction of negatively stained micrographs of the cyanide dihydratase from *B. pumilus* at a resolution of 3.2 nm. Shown are the views down the twofold axis (A and C) and a view perpendicular to the twofold axis (B). The structure is a spiral of two turns from end to end, having 18 subunits.

of 1 mM and were further incubated for 4 h at 30°C with shaking prior to being harvested.

Cell lysis. For enzyme assays and protein purification, cell pellets were resuspended in 20 mM phosphate buffer–100 mM NaCl (pH 7.8) and disrupted in a French press cell three times at 1,000 lb/in^2. The insoluble material was removed by centrifugation at 10,000 × *g* for 10 min. For small-scale preparations, cell pellets from 1 ml of induced MB2890, MB2899, or MB3033 cultures were resuspended in 100 to 500 μl of 200 mM morpholinepropanesulfonic acid (MOPS)–200 mM NaCl (pH 7.6). The resuspended pellet was then incubated at 37°C for 20 min with 2 mg of lysozyme/ml. Deoxycholate was added to 0.1%, and the samples were kept on ice for 15 min. The soluble cytosolic fraction was separated from the insoluble material in a microcentrifuge.

SDS-PAGE. Discontinuous SDS-PAGE was performed using a 15% polyacrylamide resolving gel. When running whole-cell fractions, 1 ml of cell culture was centrifuged, and the pellet was resuspended in 100 μl of SDS-reducing buffer and boiled, and 10 to 20 μl was loaded on the gel. When comparing soluble and insoluble fractions of a cell lysate, samples representing equal original cell volumes of both soluble and insoluble fractions were prepared. The gels were stained with Coomassie brilliant blue as previously described (26).

Purification of recombinant cyanide dihydratase. The six-His-tagged cyanide dihydratase enzyme was purified from crude cell lysates by immobilized nickel ion adsorption chromatography employing a 5-ml HiTrap metal chelating column (Amersham Pharmacia Biotech, Piscataway, N.J.). The 5-ml HiTrap column was charged with 2.5 ml of 0.1 M $NiSO_4$. After the soluble lysate was passed through the charged HiTrap column, it was washed with 10 column volumes of start buffer consisting of 20 mM sodium phosphate (pH 7.8), 100 mM NaCl, and 10 mM imidazole, followed by 10 column volumes of start buffer containing 100 mM imidazole. The bound protein was eluted using start buffer containing 500 mM imidazole. Fractions of 8 to 10 ml were collected and assayed for cyanide-degrading activity. Active fractions were pooled and checked for purity by SDS-PAGE. To change buffer and remove the imidazole, the pooled sample was dialyzed against 100 mM NaCl–50 mM MOPS (pH 7.6). The purified protein was stored in 30% glycerol at −80°C. Protein concentration was determined by the method of Bradford (2).

Assay for cyanide-degrading activity and kinetic analysis. Cyanide concentrations were measured by a picric acid-based method (10). To detect cyanide-degrading activity in *B. pumilus* or *E. coli* strains, 1 ml of a bacterial culture was incubated with 100 μl of 0.2 M KCN (in 0.2 M Tris base [pH 8]) at 37°C for a designated time between 0 min and overnight. After incubation, the cells were pelleted, and 100 μl of the supernatant was added to 200 μl of the picric acid assay solution (0.5% picric acid in 0.25 M sodium carbonate). This was immediately placed in a 100°C heating block for 6 min. The solution was then diluted with 700 μl of distilled H_2O, and the absorbance at 520 nm was measured. The concentration of cyanide remaining in the solution was determined by comparison with a standard curve for cyanide at concentrations between 0 and 4 mM. For concentrations greater than 4 mM, the assay supernatant was diluted so that the absorbance at 520 nm remained below 1.0.

For determination of K_m and V_{max}, 1-ml reactions were run in triplicate using enzyme diluted in 170 mM MOPS–90 mM NaCl (pH 7.6). Reaction mixtures without KCN and a 20 mM KCN solution (in 170 mM MOPS–90 mM NaCl [pH 7.6]) were prewarmed for 15 min at 37°C prior to the start of the reaction. The appropriate amount of the buffered 20 mM KCN solution was then added to the reaction mixture, and 200-μl samples were taken after 1 and 6 min. Changing the ratio of reaction mixture to picric acid solution from 1:2 to 2:1 allowed for the detection of cyanide at lower concentrations while maintaining a linear relationship between the cyanide concentration and absorbance at 520 nm. Immediately after removal, the 200-μl sample was added to 100 μl of picric acid solution, and this was incubated at 100°C for 6 min and then immediately diluted with 700 μl of H_2O and placed on ice for 15 min. The absorbance at 520 nm was taken and compared to the standard curve.

Phylogeny. A ClustalW 1.7 multiple sequence alignment (15) was made for the amino acid sequences of the cyanide dihydratases of *B. pumilus* C1 and *P. stutzeri* AK61, six known and two predicted prokaryotic nitrilases, and three of the fungal cyanide hydratases. The following parameters were used for the multiple alignment: matrix, blosum; gap opening penalty, 10.0; gap extension penalty, 0.05; hydrophilic gaps, on; hydrophilic residues, GPSNDQERK; residue-specific gap penalties, on. Phylogenetic trees were constructed with MEGA (18). Neighbor-joining and UPGMA (unweighted pair group method using arithmetic averages) trees were constructed by using various distance methods, including Poisson correction, number of differences, *P* distance, and gamma distance, and these trees were compared with trees constructed by the maximum parsimony method. All trees underwent bootstrapping with a replicate number of 500.

RESULTS

Quaternary structure determined by three-dimensional reconstruction from electron micrographs of negatively stained protein. Electron micrographs of the cyanide dihydratase at pH 8.0 published by Meyers et al. (20) showed a variety of shapes having dimensions of approximately 9 by 20 nm and occasional toroids with an outer diameter of 9 nm. The structures were described as tightly packed spirals that sometimes associated end to end to form rods of up to 50 nm in length. Three-dimensional reconstruction at a resolution of 3.2 nm shows the structure to be an irregular, but twofold symmetric, spiral of two turns having 18 distinct density peaks along its length (Fig. 2). The pitch of the spiral is approximately 8 nm, and the particle has an overall length of 18.5 nm and an outer diameter of 9.5 nm.

pH dependence of the quaternary structure. The short cyanide dihydratase spirals remain as discrete particles over the pH range from 6.0 to 8.0 (Fig. 3A) but associate to form long rods at pH 5.4 (Fig. 3B). The diameter of the rods is 13 nm,

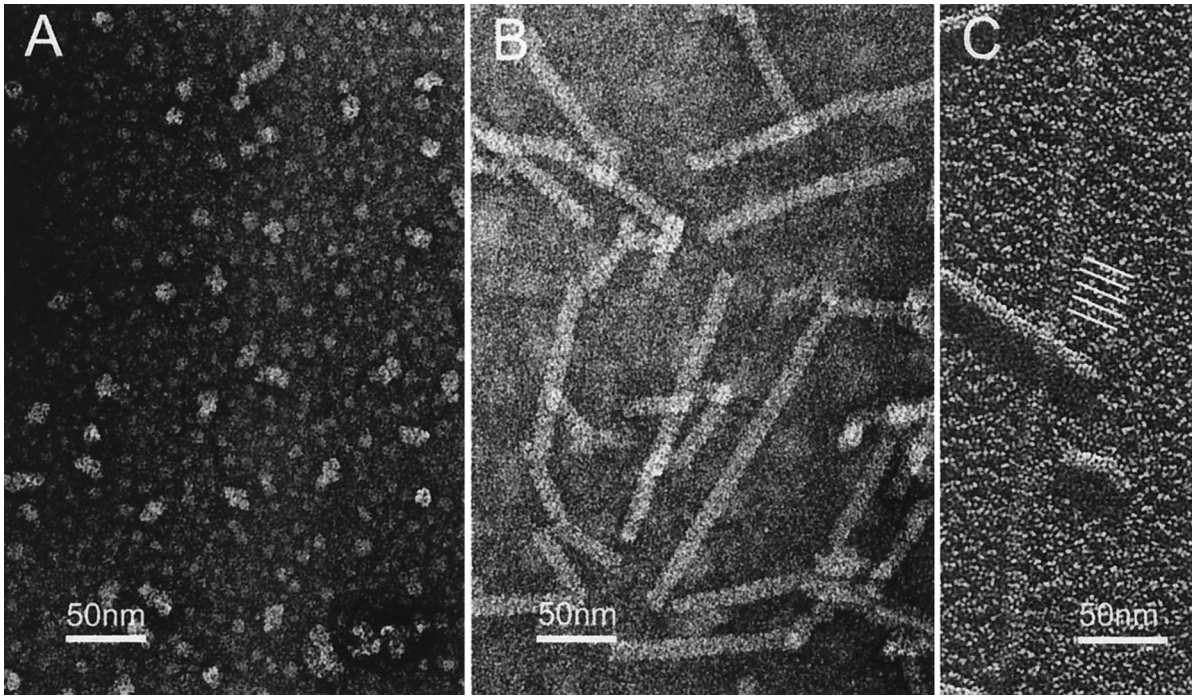

FIG. 3. Negative-stain electron micrographs of the isolated cyanide dihydratase from *B. pumilus* at pH 8.0 (A) and 5.4 (B) illustrating the transition from discrete particles to extended rods. (C) Platinum-carbon shadowing of the cyanide dihydratase rods. Regular striations along the length of the rod can be seen in rods lying parallel to the direction of shadowing. The angle of the striations implies that the helical arrangement of subunits is left handed. The location of five of the striations is emphasized by white lines.

and they have a periodicity of 8 nm along their length. Unidirectional shadowing of the rods from favorable angles shows that the ridges exposed on the outside of the rod run from lower right to top left, indicating that the path followed by the subunits is a left-handed helix (Fig. 3C).

Glutaraldehyde cross-linking and SDS-PAGE. Cross-linking the cyanide dihydratase at pH 8 with glutaraldehyde at a range of concentrations produces three dimer bands, a very weak trimer area, and a single tetramer band (Fig. 4). The three dimer bands imply that contacts between subunits in the spiral are such that dimers can form as a result of cross-linking in three different ways. The virtual absence of trimers implies that cross-linking at one of the dimer interfaces is preferred; thus, forming an additional cross-link to an already existing dimer results in the formation of a tetramer. A possible topology which would give rise to this behavior is shown in Fig. 5. In addition, the fact that one of the dimers lies on the twofold axis, as can be seen from Fig. 2C, suggests that the dimer having the topology depicted in Fig. 5 (dimer i) is the repeating unit of the spiral which grows by the addition of dimers in each of the twofold-related directions.

Determining the sequence of the cyanide dihydratase. Alignments of the partial N-terminal sequence data available for the *B. pumilus* C1 enzyme (21), the *A. xylosoxidans* subsp. *denitrificans* cyanide dihydratase (12), and the complete amino acid sequence of the *P. stutzeri* AK61 cyanide dihydratase (33) showed that these sequences are highly conserved at the amino acid level. It was therefore hypothesized that the cyanide dihydratase of *B. pumilus* C1 would share some segments of amino acid identity with the *P. stutzeri* AK61 cyanide dihydratase.

The mass spectrum of the MALDI-TOF analysis of fragments generated by a trypsin digest of purified cyanide dihydratase from *B. pumilus* C1 indicated 21 fragments, the masses of which matched predicted trypsin fragments from the *P. stutzeri* cyanide dihydratase sequence to within 0.05%. One such fragment in the *P. stutzeri* cyanide dihydratase contains the amino acid sequence AAAVQAAPVY, and this sequence was used to design the degenerate oligonucleotide primer Pum-7 (Table 2). In addition, the primer Int-1 was designed from the amino acid sequence EQVHVAAWP, which is identical in both the *P. stutzeri* cyanide dihydratase and *F. lateritium* cyanide hydratase sequences and which we therefore supposed would also be conserved in *B. pumilus*.

PCR using the degenerate primers Int-1 and Pum-7 produced a product of approximately 550 bp. This PCR product was cloned into the *Eco*RV site of pBS(KS+) to generate p3019, and its sequence was determined. It had an open reading frame over its 539-bp length that shared 86% identity at the amino acid level to the cyanide dihydratase of *P. stutzeri* AK61.

The 539-bp sequence was then used to design primers so that inverse PCR could be used to clone and sequence the flanking regions of the gene. *B. pumilus* C1 genomic DNA was digested with *Taq*I and religated at a low DNA concentration to favor intramolecular circularization of the individual *Taq*I fragments. Using the ligated product as a source of template DNA with the primers Out-2 and Out-3 (Table 2), a PCR product of approximately 1,100 bp was generated. This PCR

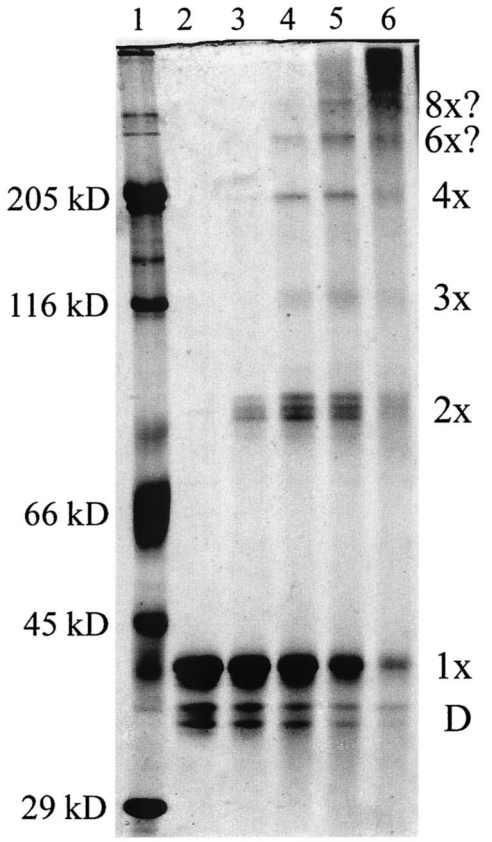

FIG. 4. SDS-polyacrylamide gel showing the effect of cross-linking the cyanide dihydratase from *B. pumilus* with glutaraldehyde. Lane 1, molecular mass markers: carbonic anhydrase (29 kDa), ovalbumin (45 kDa), bovine serum albumin (66 kDa), beta-galactosidase (116 kDa), and myosin (205 kDa). Lane 2, un-cross-linked cyanide dihydratase. The two contaminating bands (D) are probably proteolytic degradation products which arise because phenylmethylsulfonyl fluoride cannot be used as a protease inhibitor in the preparation of the enzyme, as it interferes with the cyanide assay. Lanes 3 to 6, enzyme cross-linked with 0.002, 0.005, 0.01 and 0.02% glutaraldehyde, respectively. The locations of monomers, dimers, trimers, and tetramers are indicated. All of these bands are in the linear part of the gel and run anomalously as though the protein had a molecular mass of 43 kDa. The bands putatively assigned as hexamers and octamers are in the nonlinear part of the gel. The presence of three dimer bands, a very weak trimer region, and a single tetramer band has implications for the arrangement of the subunits in the spiral, which are discussed in the caption to Fig. 5.

product was cloned into the *Eco*RV site of pBS(KS+) and sequenced to about 200 nucleotides beyond the 3′ end of the putative cyanide dihydratase gene. This DNA contained an open reading frame which shared 77% amino acid identity with the cyanide dihydratase of *P. stutzeri* AK61 and lacked only the coding region for the very N terminus of the protein and the promoter.

Attempts to clone the promoter and N-terminal coding region of the cyanide dihydratase gene of *B. pumilus* C1 by inverse PCR with other enzymes and primer pairs were unsuccessful. Therefore, an alternate strategy was devised to disrupt the native gene and clone the adjacent DNA. The plasmid p3022 (consisting of the temperature-sensitive *Staphylococcus aureus* plasmid pE194 cloned into the *Sac*I and *Pst*I sites of p3019) was transformed into *B. pumilus* C1 to generate strain MB3025 (Fig. 6). Homologous recombination-based gene disruption of the *B. pumilus* C1 cyanide dihydratase gene was selected by growing at 51°C, the temperature at which the plasmid fails to replicate, to generate strain MB3025-1. The 539-bp internal fragment acts as a region of homology, thereby generating an insertion of the whole plasmid within the cyanide dihydratase gene. Strain MB3025-1 failed to exhibit cyanide degrading activity, confirming that the relevant gene had been disrupted.

The integrated plasmid, as well as flanking DNA, was then rescued by digesting the genomic DNA of the integrant with *Sac*I, religating, transforming into *E. coli*, and selecting on ampicillin. By this strategy, the flanking DNA, which consisted of the upstream and N-terminal coding region of the cyanide dihydratase gene, was rescued. This was further substantiated, as the first seven codons of the putative open reading frame agreed with N-terminal sequence data generated from purified enzyme (20) and overlapped with the previous gene fragments. The final sequence (GenBank accession no. AF492815) revealed an open reading frame encoding 330 amino acids (Fig. 7) that shared 80% identity and 91% similarity with the putative amino acid sequence of the cyanide dihydratase of *P.*

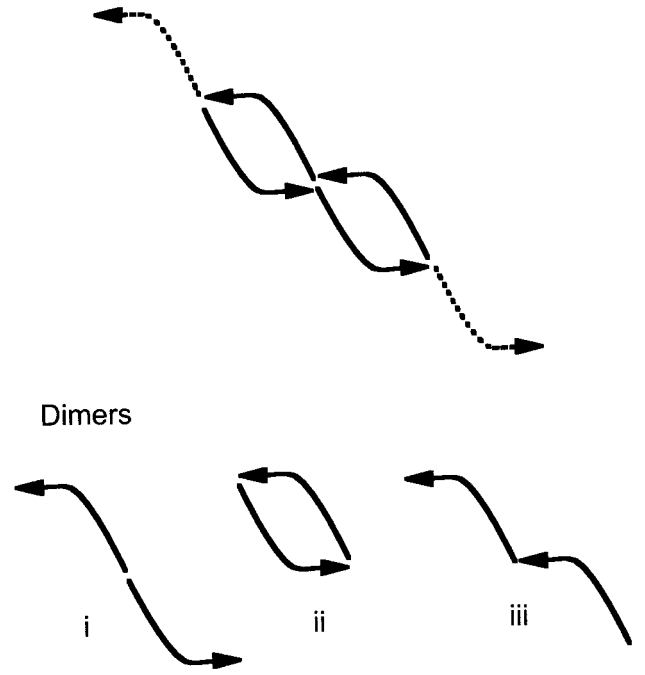

FIG. 5. A possible topology which would lead to a spiral arrangement having twofold symmetry and which could cross-link to form three different dimer arrangements and only one possible tetramer. The asymmetric arrows represent simplified subunits of unknown shape, proximity gives rise to the possibility of cross-links, and there is no relationship to the directionality of the polypeptide chain or the location of the cross-link within the polypeptide. If cross-links formed preferentially across one interface, then this arrangement would also explain the absence of a trimer band and the formation of a single tetramer band. Illustrated is the preferred twofold symmetric dimer (i), the addition of which would lead to the elongation of the spiral and would give rise to the twofold symmetry of the complex. The other two possibilities (ii and iii) for dimer formation implied by our suggested topology are also shown.

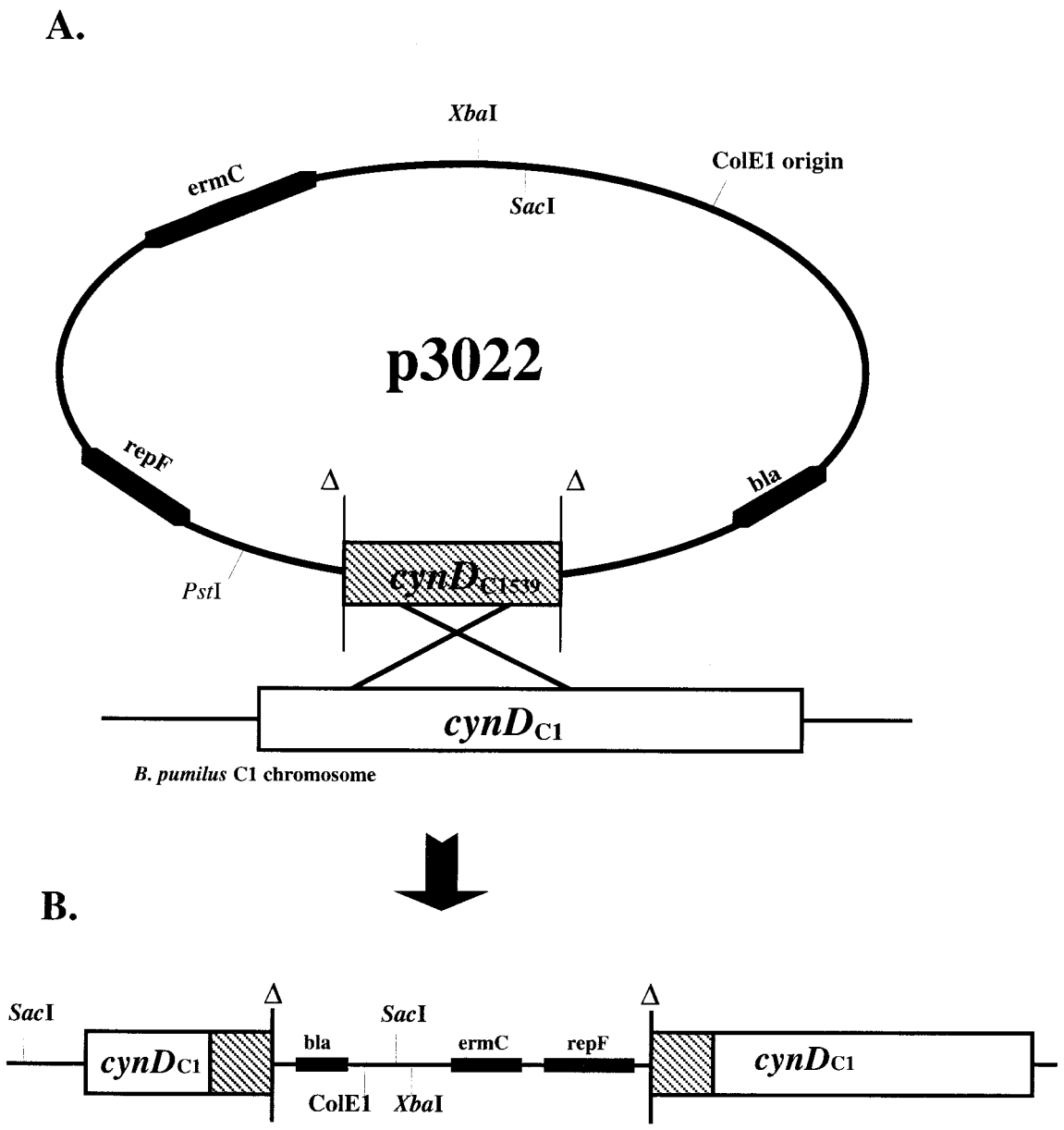

FIG. 6. Homologous recombination in *B. pumilus* C1 using p3022. The hybrid plasmid p3022 was made by cloning p3019 into the *Xba*I and *Pst*I sites of pE194. This plasmid was designed to be used as a temperature-sensitive shuttle plasmid for *Bacillus* and *E. coli*. The *bla* gene encodes ampicillin resistance for selection in *E. coli*, and *ermC* encodes erythromycin resistance for selection in *Bacillus*. The $cynD_{539}$ encodes the partial 539-bp PCR product from the putative cyanide dihydratase of *B. pumilus* C1. *B. pumilus* C1 was transformed with p3022 to make strain MB3025. This diagram shows p3022 integration into the cyanide dihydratase gene of *B. pumilus* C1 by homologous recombination. (A) Recognition of homologous regions of p3022 with the gene encoding cyanide dihydratase. (B) The integrated plasmid p3022 flanked by the gene encoding cyanide dihydratase. The gene encoding replication initiation protein for plasmid replication in *Bacillus* species, *repF*, is also shown. The origin of plus-strand synthesis, ori^+, is not shown but is located within the *repF* gene.

stutzeri AK61. Despite sharing a high degree of similarity on the amino acid level with the cyanide dihydratase of *P. stutzeri* AK61, there was only 43% identity at the DNA level.

Cloning and expression of the cyanide dihydratase gene in *E. coli*. Based on the DNA sequence data, primers were designed for cloning the cyanide dihydratase gene of *B. pumilus* C1 into the *Nde*I and *Xho*I sites of pET26b. PCR products of the cyanide dihydratase gene were generated with the two different 3′ primers. The primer Pum-*Xho*I (Table 2) was designed to include the stop codon; however, primer Pum-His was designed to delete the TAA stop codon so that upon insertion of the Pum-His-derived PCR product into the *Nde*I and *Xho*I sites of pET26b, a genetic fusion would be created between the open reading frame of the cyanide dihydratase gene and the six-histidine codon tag at its C terminus in pET26b. PCR products with the aforementioned primers were cloned as blunt-ended fragments into the *Eco*RV site of pBS (KS+), from which they were sequenced to verify there were no PCR-induced mutations. The cyanide dihydratase gene was then subcloned into the *Nde*I and *Xho*I sites of pET26b. Since

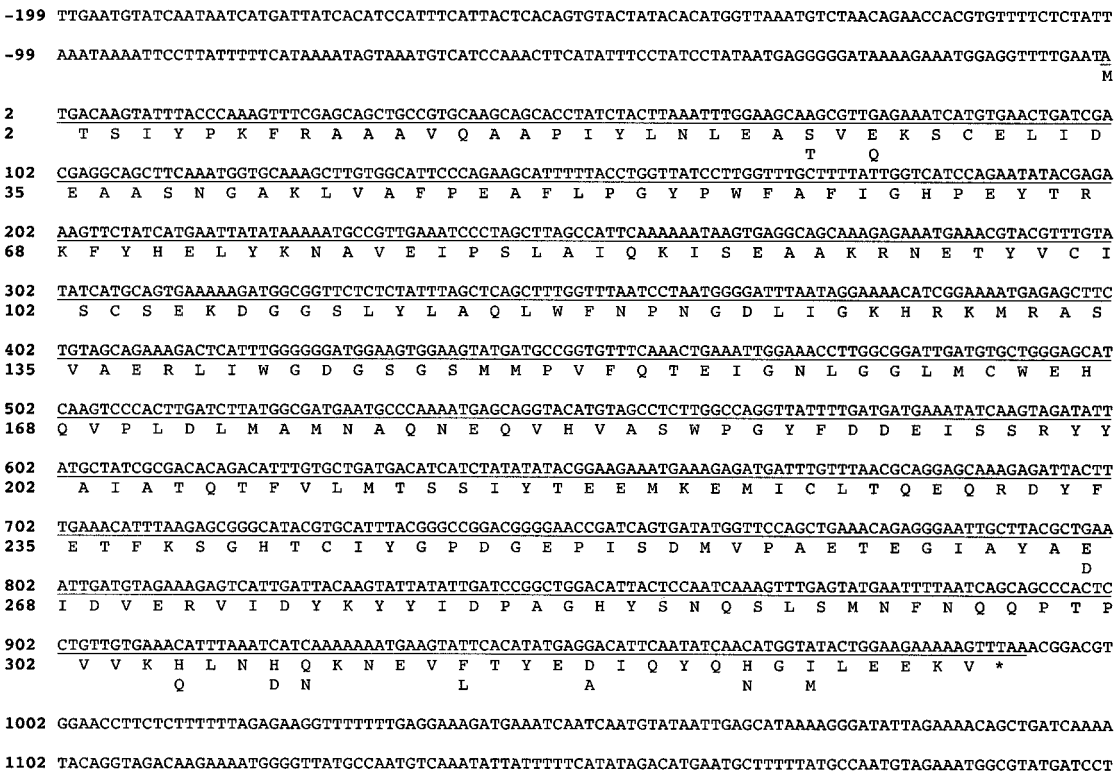

FIG. 7. DNA sequence of the *cynD* gene encoding cyanide dihydratase in *B. pumilus* C1 (GenBank accession no. AF492815) with the deduced amino acid sequence shown below. Those amino acid residues which differ for the *B. pumilus* 8A3 CynD (GenBank accession no. AF492814) are denoted underneath the corresponding *B. pumilus* C1 CynD amino acid sequence.

the gene encoding cyanide dihydratase has an internal *Nde*I restriction site, a partial *Nde*I digest was used to isolate the full-length gene prior to its insertion into pET26b. These plasmids were transformed into the *E. coli* strain BL-21(DE3) pLysS to generate strains MB2890 and MB2899, respectively. Both strains demonstrated the ability to degrade cyanide after IPTG induction.

The cyanide-degrading activities of strains MB2890 and MB2899 were compared to ascertain whether the six-His tag affects the activity or expression of the recombinant cyanide dihydratase. There was no detectable difference between the relative activities of crude lysates from strains MB2890 and MB2899, suggesting that little or no activity is lost with the addition of a C-terminal 6-His tag.

A rapid screen was performed to determine the optimal temperature for cyanide dihydratase expression in *E. coli*; cultures of strain MB2890 were induced separately at temperatures of 22, 30, and 37°C for 4 h. SDS-PAGE was used to compare the relative levels of cyanide dihydratase present in the soluble and insoluble lysate fractions (Fig. 8). Growth at both 30 and 37°C generated similar levels of CynD expression, which was significantly higher than that observed at 22°.

The cyanide dihydratase was purified by nickel resin affinity chromatography as described, and SDS-PAGE was used to analyze the purity of the protein preparation. The preparation appeared to be homogeneous (Fig. 8, lane 10). From this gel, one can also observe that much of the CynD protein is present in the insoluble fraction. To ascertain whether the recombinant strain had greater cyanide-degrading potential than the wild-type *B. pumilus* C1, the activities of the cell lysate from MB2890 were compared with that previously reported for *B. pumilus* C1 (20). The recombinant *E. coli* strain had noticeably higher activity (Table 3). Affinity-purified cyanide dihydratase from strain MB2899 was also included for comparison.

Kinetic analysis showed that the recombinant enzyme had a K_m of 7.0 mM for cyanide and a V_{max} of 97 μmol min^{-1} mg^{-1}, compared to the published results of 2.5 mM and 88 μmol min^{-1} mg^{-1} (data are from reference 20 but are converted to comparable units).

Cyanide dihydratase in other strains of *B. pumilus*. Is *B. pumilus* strain C1 unique, perhaps due to selection at its site of origin, or is the cyanide dihydratase found in other *B. pumilus* strains? To test this, we attempted to amplify this gene from a wild-type isolate of *B. pumilus* (Bacillus Genetic Stock Collection BGSC 8A3 or ATCC 7061) with the primers Pum-*Nde*I and Pum-*Xho*I. *B. pumilus* 8A3 does not express detectable levels of cyanide dihydratase when grown overnight at either 30 or 37°C in LB broth. Supplementing the media with $MnCl_2$ did not induce cyanide-degrading activity, as it does for *B. pumilus* C1. However, the PCR of 8A3 genomic DNA succeeded in amplifying a DNA fragment approximately the size of that amplified from *B. pumilus* C1. The PCR product was subsequently cloned into the *Nde*I and *Xho*I sites of pBS(KS+). DNA sequencing revealed an open reading frame (GenBank accession no. AF492814) which was 92% identical on the DNA level with the gene encoding cyanide dihydratase in *B. pumilus* C1. The predicted proteins differ by only 10 amino acids, of which two differences are near the N terminus

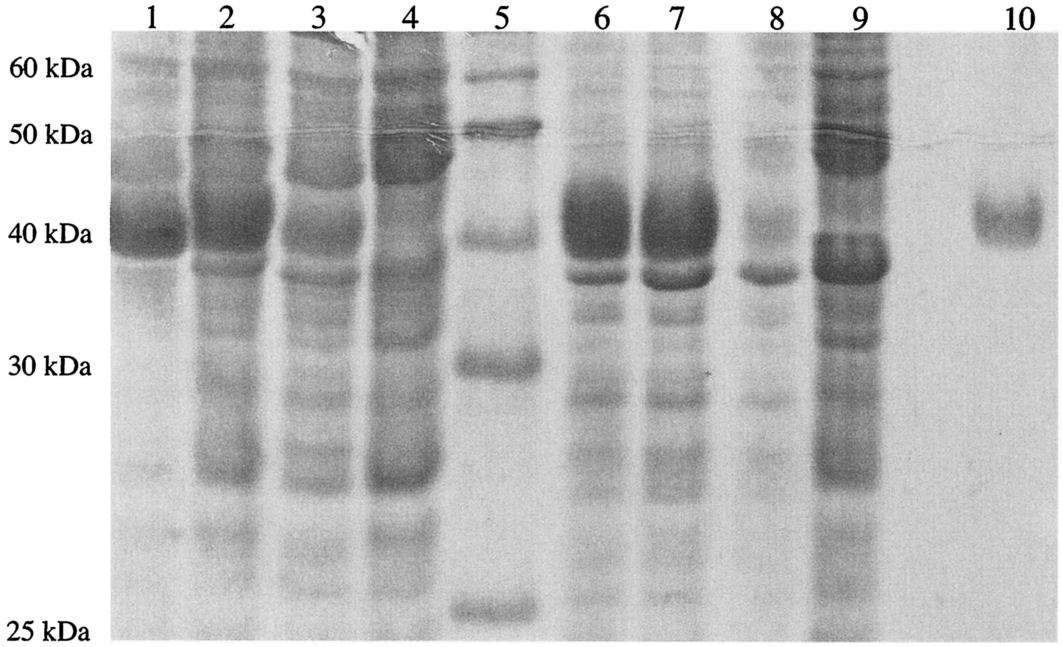

FIG. 8. SDS-PAGE of cell lysates showing the soluble (lanes 1 to 3) and insoluble (lanes 6 to 8) fractions from MB2890 cultures induced at 37, 30, and 22°C, respectively. Lanes 4 and 9 are, respectively, the soluble and insoluble fractions of a lysate from an uninduced culture grown at 37°C. In lane 5 are molecular mass markers. Lane 10 is the His-tagged cyanide dihydratase from MB2899 obtained by affinity purification.

and the remainder cluster at the C terminus. The differences are shown in Fig. 7. Immediately beyond the coding sequence, a 198-bp insertion exists in the 8A3 sequence, and then the sequence identity (87%) resumes. We do not have sequence data upstream of the 8A3 coding region.

This gene was subcloned into pET26b and transformed into *E. coli* BL-21(DE3) pLysS for expression. Following induction, cell lysates from this strain (MB3033) had cyanide-degrading activity comparable to lysates of MB2890 and MB2899, suggesting that although the cyanide dihydratase gene is functional in *B. pumilus* 8A3, it most likely is not expressed; however, formally, it could merely be regulated differently than *cynD* of *B. pumilus* C1 or could be coexpressed with an inhibitor.

Phylogenetic comparison of *B. pumilus* C1 cyanide dihydratase with other cyanide dihydratases, cyanide hydratases, and non-cyanide-degrading nitrilases. A phylogenetic comparison of *B. pumilus* C1 cyanide dihydratase was made with other cyanide dihydratases, cyanide hydratases, and non-cyanide-degrading nitrilases by constructing phylogenetic trees (Fig. 9) using MEGA (18). The non-cyanide-degrading nitrilases chosen were those prokaryotic enzymes most closely related to CynD based on a Blastx search, while the cyanide-degrading hydratases of fungal origin were chosen because they shared similarity with other nitrilases and hydrolyzed cyanide. Multiple trees were made by using various methods and parameters, but the phylogenetic relationships among the cyanide dihydratases with the other enzymes were consistent in the various analyses. For these trees, the neighbor-joining tree (Fig. 9) is representative. As seen in Fig. 9, the cyanide dihydratases group most closely with the nitrilases of *Bacillus* sp. strain Oxb-1 and *Comamonas testosteroni* strain JC4212. In addition, the fungal cyanide hydratases do not appear to be any more related to the cyanide dihydratases than are the aliphatic nitrilases of *Rhodococcus rhodochrous* and *Klebsiella pneumoniae* subsp. *ozaenae*. As these cyanide hydratases are eukaryotic in origin, it is reasonable to speculate that their ability to catalyze cyanide hydration may have arisen convergently from a closely related nitrilase. Alternatively, there is no evidence to dismiss the possibility that these enzymes evolved via divergence from a common cyanide-degrading nitrilase.

DISCUSSION

Cyanide dihydratases readily convert cyanide to relatively nontoxic products, do not require any cofactors, and do not have any known ancillary substrates (20). These qualities make CynD a candidate for use in the detoxification of cyanide-containing industrial waste waters. Despite their potential commercial value, there is limited knowledge concerning the structure-function relationship of these enzymes. *cynD* of *B. pumilus* C1 represents only the second cyanide dihydratase gene to have ever been cloned and sequenced, and it is the first of the three known cyanide dihydratases to have its quaternary structure described.

TABLE 3. Enzyme activities

Sample	Total protein (mg)	Total activity (U)	Sp act (U/mg)
B. pumilus C1[a]	225	272.9	1.2
MB2890	212.1	2,804	13.2
His-purified MB2899	17.3	2,336	135

[a] Data of Meyers et al. (20) for the cell lysate.

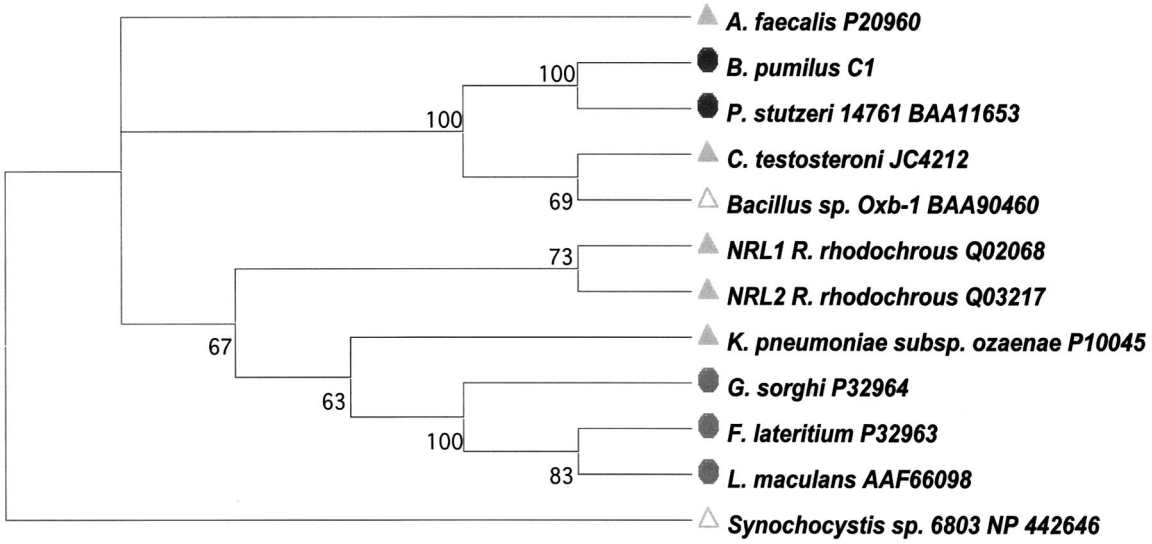

FIG. 9. Neighbor-joining phylogenetic tree of cyanide-specific and -nonspecific nitrilases. The enzymes are listed according to their host and accession number and are grouped as follows: ●, cyanide dihydratase or cyanide-specific nitrilases; ▲, aliphatic nitrilases; △, putative nitrilases for which the substrate has not yet been determined; ◍, cyanide hydratases of fungal origin.

The gene *cynD* encodes the cyanide dihydratase previously described in *B. pumilus* C1 (19). The high level of identity shared on the amino acid level with the cyanide dihydratase of *P. stutzeri* AK61, the ability to express cyanide degradation in *E. coli*, and the loss of the cyanide-degrading activity of *B. pumilus* C1 by gene disruptions together suggest that it is the sole gene encoding cyanide dihydratase in *B. pumilus* C1.

Originally, it was proposed that the cyanide dihydratase of *B. pumilus* C1 was composed of three subunits of slightly different molecular weights, but N-terminal amino acid sequencing suggested that there was only one N terminus common to all three subunits (20, 21). Upstream sequence analysis shows four possible translational start sites, although only one that would begin with the aforementioned N terminus. This start site is also the only one carrying a sequence matching a consensus good ribosome binding site. In addition, expression of *cynD* in *E. coli* using this start codon allows for production of an enzyme which behaves similar to that reported for *B. pumilus* C1. Finally, polyacrylamide gels of untagged *E. coli*-expressed product reveal the same three bands as the wild-type enzyme, but the degradation bands are of much less intensity than the full length (data not shown). We therefore conclude that these three bands are the result of either proteolytic cleavage or some other posttranslation modification of a single gene product.

The ability to produce CynD in *E. coli*, along with being able to purify it by using an affinity six-histidine tag, greatly facilitates its potential for use on an industrial level. Recombinant cyanide dihydratase appeared to be similarly active as the native protein purified from *B. pumilus* C1. The level of activity of crude MB2890 lysates induced for 4 h was 10-fold that reported for *B. pumilus* C1 extracts prepared from cells grown overnight under optimal conditions for *cynD* expression. The addition of the six-His tag, while facilitating purification, did not appear to alter the activity of the enzyme. The structure of both the His-tagged and untagged recombinant enzymes appeared similar to the native enzyme by negative-stain electron microscopy at pH 8.0. The pH 5.4 structural transition was observed in the case of the untagged recombinant enzyme, but the His-tagged recombinant enzyme was not tested.

Analysis by gel filtration chromatography suggested that the native enzyme is in the form of multimers larger than 300 kDa, but it has not been proven whether multimer formation is required for enzyme activity (20, 21). Experiments to alter multimer formation are under way.

Results from negative-stain electron microscopy suggest that the enzyme assumes a spiral structure of 18 subunits at pH 8, consistent with the size determined by light-scattering experiments (unpublished results). Thus, the total molecular mass of the complex is 672 kDa. The cross-linking study and the twofold symmetry suggest that the spiral is built up from a dimer building block. The reason for the termination of the spiral at 18 subunits at pH 8 is not apparent at the resolution attained, but it is suspected to be due to distortion of the helical symmetry. A transition from short spirals to long helices happens as the pH drops below 6.0. This structural change implicates a histidine which has a pK_a of 6.0. It is proposed that when an as-yet-unidentified histidine acquires a charge, it forms an ionic bond with a neighboring acidic residue, and the energy from this interaction drives the observed structural change. We propose that the structural change that occurs at the subunit level is fairly small, for example, a small change in the angle of association of the subunits which allows the short spirals to associate and thus form the extended helices. As we believe that no major rearrangement occurs during the structural transition, we propose further that the short spirals are also left handed.

The ability to express cyanide dihydratase activity may be a characteristic of *B. pumilus* strains in general. In this paper, we demonstrate that a wild-type isolate of *B. pumilus* (BGSC 8A3) that appeared to be negative for cyanide-degrading activity actually carried a gene that encoded functional cyanide dihy-

dratase when expressed in *E. coli*. Therefore, it is unlikely that the cyanide-degrading activity of strain C1 was the result of selection for a novel gene product at a cyanide-contaminated site. Other cyanide-degrading isolates of *B. pumilus* have been isolated (28), as well as strain VWO, recently isolated from noncontaminated soil in Cape Town.

It was demonstrated that lag-phase and exponential-phase *B. pumilus* C1 cultures were unable to degrade cyanide, while cyanide-degrading activity was present in cultures undergoing late exponential and stationary phase (19). Since sporulation is an event which occurs during the latter phases of growth in *Bacillus* spp., the expression of cyanide dihydratase and the onset of sporulation may therefore have common regulatory components. In fact, mutagenesis experiments in *B. pumilus* C1 using the transposon *Tn*917 yielded a number of mutants no longer able to degrade cyanide. DNA sequencing of the *Tn*917 insertion sites showed that many of the corresponding mutations were in *spoOA* (14), and all of the mutants with such mutations failed to sporulate, suggesting that *cynD* may be regulated by *spoOA*, either directly or indirectly. This is further supported by the observation that *B. pumilus* strain 8A3 neither sporulated nor degraded cyanide under the selected growth conditions. Together, these observations may be taken to imply that there is a link between cyanide dihydratase expression and at least some genes regulated with sporulation. In *B. subtilis*, the gene product SpoOA encodes a transcription factor which regulates a myriad of genes associated with late growth functions and response to nutrient depletion. Examples of developmental events regulated by SpoOA are the onset of sporulation, induction of competence, and production and secretion of antibiotics and extracellular proteases.

The role of cyanide dihydratase in stationary-phase cells is an interesting question. Thousands of species of plants are cyanogenic, suggesting that the ability to degrade cyanide may enhance the survival of some plant symbionts. Such a proposal has previously been made in order to explain the role of cyanide hydratase activity in *G. sorghi* pathogenesis (31). *B. pumilus* has also been implicated as a symbiont in the promotion of plant growth and protection against plant pathogens (30).

In conclusion, the gene encoding cyanide dihydratase in *B. pumilus* C1 has been cloned and sequenced. The putative amino acid sequence is about 80% identical to that of the cyanide dihydratase of *P. stutzeri* AK61, and it is not significantly more related to cyanide hydratases than it is to other nitrilases, thereby supporting its classification as a cyanide-specific nitrilase. The defined-length spiral quaternary structure at the pH optimum possibly represents a novel form of structural organization which is characteristic of this class of enzymes; it is the first example of a self-terminating spiral structure protein that we are aware of. This deserves further investigation. The ability to express the cyanide dihydratase gene in *E. coli* at high levels, along with one-step purification by affinity chromatography, makes it a superb candidate for use in industrial processes for the removal of cyanide from cyanide-containing waste.

ACKNOWLEDGMENTS

The first two authors contributed equally to this work and should be considered as co-first authors.

We gratefully acknowledge the Robert A. Welch Foundation, the University of Houston Environmental Institute, and the Gulf Coast Hazardous Substance Research Center (no. 069UHH0789) to M.J.B. for support of this project. M.B. received financial assistance from the National Research Foundation, and B.T.S. received financial assistance from the Wellcome Trust.

B.T.S. and M.B. are grateful for assistance received from Wolf Brandt, Anke Fiedler, Mohamed Jaffer, Paul Chang, James Duncan, Dennis Burford, and Brendon Price.

REFERENCES

1. **Birnboim, H., and J. Doly.** 1979. A rapid alkaline extraction procedure for screening recombinant plasmid DNA. Nucleic Acids Res. **7:**1513–1523.
2. **Bradford, M.** 1976. A rapid and sensitive method for the quantification of microgram quantities of protein utilizing the principle of protein-dye binding. Anal. Biochem. **72:**248–254.
3. **Bron, S.** 1990. Plasmids, p. 15–174. *In* C. R. Harwood and S. M. Cutting (ed.), Molecular biological methods for *Bacillus*. John Wiley & Sons, Inc., New York, N.Y.
4. **Burkholder, P. R., and N. H. Giles.** 1947. Induced biochemical mutations in *Bacillus subtilis*. Am. J. Bot. **34:**345–348.
5. **Cluness, M. M., P. D. Turner, E. Clements, D. T. Brown, and C. O'Reilly.** 1993. Purification and properties of cyanide hydratase from *Fusarium lateritium* and analysis of corresponding *chyI* gene. J. Gen. Microbiol. **139:**1807–1815.
6. **Crowther, R. A., R. Henderson, and J. M. Smith.** 1996. MRC image processing programs. J. Struct. Biol. **116:**9–16.
7. **Cutting, S. M., and P. B. Vander Horn.** 1990. Genetic analysis, p. 27–74. *In* C. R. Harwood and S. M. Cutting (ed.), Molecular biological methods for *Bacillus*. John Wiley & Sons, Inc., New York, N.Y.
8. **Dubey, S. K., and D. S. Holmes.** 1995. Biological cyanide destruction mediated by microorganisms. World J. Microbiol. Biotechnol. **11:**257–265.
9. **Dubnau, D., and R. Davidoff-Abelson.** 1971. Fate of transforming DNA following uptake by competent *Bacillus subtilis*. 1. Formation and properties of the donor-recipient complex. J. Mol. Biol. **56:**209–221.
10. **Fisher, F. B., and J. S. Brown.** 1952. Colorimetric determination of cyanide in stack gas and waste water. Anal. Chem. **24:**1440–1444.
11. **Frank, J., M. Radermacher, P. Penczek, J. Zhu, Y. Li, M. Ladjadj, and A. Leith.** 1996. SPIDER and WEB: processing and visualization of images in 3D electron microscopy and related fields. J. Struct. Biol. **116:**190–199.
12. **Ingvorsen, K., B. Højer-Pedersen, and S. E. Godtrfedsen.** 1991. Novel cyanide-hydrolyzing enzyme from *Alcaligenes xylosoxidans* subsp. *denitrificans.* Appl. Environ. Microbiol. **57:**1783–1789.
13. **Ingvorsen, K., S. E. Godtfredsen, B. Højer-Pedersen, and Novo Nordisk.** May 1992. Microbial cyanide converting enzymes, their production and use. U.S. patent 5,116,744.
14. **Jandhyala, D. M.** 2003. Ph.D. dissertation. University of Houston, Houston, Tex.
15. **Jeanmougin, F., J. D. Thompson, M. Gouy, D. G. Higgins, and T. J. Gibson.** 1998. Multiple sequence alignment with Clustal X. Trends Biochem. Sci. **23:**403–405.
16. **Knowles, C. J.** 1976. Microorganisms and cyanide. Bacteriol. Rev. **40:**652–680.
17. **Knowles, C. J.** 1988. Cyanide utilization and degradation by microorganisms, p. 3–15. *In* D. Evered and S. Harnett (ed.), Cyanide compounds in biology. CIBA Foundation Symposium 140. John Wiley & Sons Ltd., Chichester, United Kingdom.
18. **Kumar, S., K. Tamura, and M. Nei.** 1993. MEGA: molecular evolutionary genetics analysis, version 1.01. The Pennsylvania State University, University Park, Pa.
19. **Meyers, P. R., P. Gokool, D. E. Rawlings, and D. R. Woods.** 1991. An efficient cyanide-degrading *Bacillus pumilus* strain. J. Gen. Microbiol. **137:**1397–1400.
20. **Meyers, P. R., D. E. Rawlings, D. R. Woods, and G. G. Lindsey.** 1993. Isolation and characterization of a cyanide dihydratase for *Bacillus pumilus* C1. J. Bacteriol. **175:**6105–6112.
21. **Meyers, P. R.** 1993. Ph.D. dissertation. University of Cape Town, Cape Town, South Africa.
22. **Pace, H. C., and C. Brenner.** 2001. The nitrilase superfamily: classification, structure and function. Genome Biol. **2:**Rev.1.1–Rev.1.8.
23. **Penczek, P., M. Rademacher, and J. Frank.** 1992. Three-dimensional reconstruction of single particles embedded in ice. Ultramicroscopy **40:**33–53.
24. **Penczek, P., J. Zhu, and J. Frank.** 1996. A common-lines based method for determining orientations for N>3 particle projections simultaneously. Ultramicroscopy **63:**205–218.
25. **Richardson, K., and P. Clarke, Imperial Chemical Industries.** June 1993. Production of cyanide hydratase. U.S. patent 5,219,750.
26. **Sambrook, J., E. F. Fritsch, and T. Maniatis.** 1989. Molecular cloning: a laboratory manual, 2nd ed., p. 18.1–18.88. Cold Spring Harbor Laboratory Press, Cold Spring Harbor, N.Y.
27. **Skerman, V. B. D., V. McGowan, and P. H. A. Sneath (ed.).** 1980. Approved lists of bacterial names. Int. J. Syst. Bacteriol. **30:**225–420.

28. **Skowronski, B., and G. A. Strobel.** 1969. Cyanide resistance and cyanide utilization by a strain of *Bacillus pumilus*. Can. J. Microbiol. **15:**93–98.
29. **Solomonson, L. P.** 1981. Cyanide as a metabolic inhibitor, p. 11–28. *In* B. Vennesland, E. E. Conn, C. J. Knowles, J. Westley, and F. Wissing (ed.), Cyanide in biology. Academic Press, London, United Kingdom.
30. **Vavrina, C. S.** 1999. The effect of LS213 (B*acillus pumilus*) on plant growth promotion and systemic acquired resistance in muskmelon and watermelon transplants and subsequent field performance. Acta Hort. **504:**107–112.
31. **Wang, P., D. E. Matthews, and H. D. VanEtten.** 1992. Purification and characterization of cyanide hydratase from the phytopathogenic fungus *Gloeocercospora sorghi*. Arch. Biochem. Biophys. **298:**569–575.
32. **Watanabe, A., K. Yano, K. Ikebukuro, and I. Karube.** 1998. Cyanide hydrolysis in a cyanide-degrading bacterium, *Pseudomonas stutzeri* AK61, by cyanidase. Microbiology **144:**1677–1682.
33. **Watanabe, A., K. Yano, K. Ikebukuro, and I. Karube.** 1998. Cloning and expression of a gene encoding cyanidase from *Pseudomonas stutzeri* AK61. Appl. Microbiol. Biotechnol. **50:**93–97.
34. **Way, J. L.** 1981. Pharmacologic aspects of cyanide and its antagonism, p. 29–49. *In* E. Vennesland, E. Conn, C. J. Knowles, J. Westley, and F. Wissing (ed.), Cyanide in biology. Academic Press, London, United Kingdom.
35. **Weisblum, B., M. Y. Braham, T. Gryczan, and D. Dubnau.** 1979. Plasmid copy number control: isolation and characterization of high-copy-number mutants of plasmid pE194. J. Bacteriol. **137:**635–643.
36. **Young, C. A., and T. S. Jordan.** 1995. Cyanide remediation: current and past technologies, p. 104–129. *In* L. E. Erickson, D. L. Tillison, S. C. Grant, and J. P. McDonald (ed.), Proceedings of the 10th Annual Conference on Hazardous Waste Researchu. Kansas State University, Manhattan, Kans.